A Raman spectroscopic study of arsenite and thioarsenite species in aqueous solution at 25 °C

Scott A. Wood,*[a] C. Drew Tait[b] and David R. Janecky[b]

[a]*Department of Geological Sciences, Box 443022, University of Idaho, Moscow, ID 83844-3022, USA. E-mail: swood@uidaho.edu*
[b]*Chemical Science and Technology Division, Los Alamos National Laboratory, Los Alamos, NM 87545, USA*

Article

Received 17th December 2001, Accepted 19th February 2002
Published on the Web 26th February 2002

The Raman spectra of thioarsenite and arsenite species in aqueous solution were obtained at room temperature. Solutions at constant ΣAs + ΣS of 0.1 and 0.5 mol kg^{-1} were prepared with various ΣS/ΣAs ratios (0.1–9.0) and pH values (~7–13.2). Our data suggest that the speciation of As under the conditions investigated is more complicated than previously thought. The Raman measurements offer evidence for at least six separate S-bearing As species whose principal bands are centered near 365, 385, 390, 400, 415 and 420 cm^{-1}. The data suggest that at least two different species may give rise to bands at 385 cm^{-1}, bringing the probable minimum number of species to seven. Several additional species are possible but could not be resolved definitively. In general, the relative proportions of these species are dependent on total As concentration, ΣS/ΣAs ratio and pH. At very low ΣS/ΣAs ratios we also observe Raman bands attributable to the dissociation products of H_3AsO_3(aq). Although we were unable to assign precise stoichiometries for the various thioarsenite species, we were able to map out general pH and ΣS/ΣAs conditions under which the various thioarsenite and arsenite species are predominant. This study provides a basis for more detailed Raman spectroscopic and other types of investigations of the nature of thioarsenite species.

1. Introduction

In moderately oxidizing to moderately reducing hydrothermal solutions the species $H_3AsO_3^0$ or one of its deprotonated equivalents generally is considered to be the dominant form of dissolved arsenic.[1–9] The As(v) species $H_3AsO_4^0$ or one of its dissociation products may be predominant under near-surface, oxidizing conditions.[6,10] Under extremely reducing conditions, dissolved arsine gas, AsH_3(aq), may be an important species.[5] However, at low temperatures, in near-neutral to alkaline, sulfide-rich solutions, some form of thioarsenite [As(III)-sulfide] species is most likely responsible for the hydrothermal transport of As.[2,7,11–24]

The exact stoichiometry of the important thioarsenite complexes remains controversial even under standard conditions despite intense investigation. Spycher and Reed[21,25,26] proposed that the As(III)-sulfide species most consistent with the available literature at the time were the trimers $H_3As_3S_6^0$, $H_2As_3S_6^-$ and $HAs_3S_6^{2-}$. Krupp[27,28] emphasized some of the drawbacks of the approach of Spycher and Reed[21] and favored, in analogy with Sb, some form of the dimer ($H_2As_2S_4$, $HAs_2S_4^-$, or $As_2S_4^{2-}$). Subsequently, new experimental solubility studies have been interpreted both in terms of the trimer $H_2As_3S_6^-$[7,23] and the dimeric species.[22] Using EXAFS, Raman spectroscopy and *ab initio* molecular orbital calculations, Helz and coworkers[24] have concluded that, in solutions undersaturated with respect to either orpiment or amorphous As_2S_3, monomeric species (*i.e.*, $H_2AsS_3^-$ and $HAsS_3^{2-}$, actually formulated[24] as $AsS(SH)_2^-$ and $AsS_2(SH)^{2-}$) are predominant. However, Helz and coworkers[24] reinterpret previous solubility experiments[7,22,23] and suggest that, at saturation, the predominant species are the trimer $As_3S_4(SH)_2^-$ and the monomer $AsS(OH)(SH)^-$. Thus, the results of Helz *et al.*[24] strongly support the possibility that the degree of polymerization of thioarsenite species depends on the total As concentration in solution and that there may be a progression from monomers through dimers to trimers (to possibly higher polymers) as total As increases towards saturation with respect to an arsenic sulfide phase. Krupp[29] has suggested the possibility of a similar progression for thioantimony species.

It is apparent from this brief review of the literature that additional work is required to determine unambiguously the stoichiometries and thermodynamic stabilities of thioarsenite species. In this paper we present results of Raman spectroscopic measurements conducted on thioarsenite and arsenite species near 25 °C in near-neutral to alkaline solutions. These results are preliminary in nature but they do provide some additional constraints on the nature of thioarsenite species and the conditions under which they are transformed into arsenite species.

2. Experimental

All solution preparation and manipulation was conducted in a low-oxygen, nitrogen-filled glove bag in order to minimize oxidation. Solutions were prepared in which the total sulfur to total arsenic ratio (ΣS/ΣAs) varied but the sum of the total arsenic and sulfide concentrations was held constant. A NaHS stock solution was prepared by bubbling H_2S gas through a solution of known NaOH concentration until measured pH was constant with time. A sodium arsenite solution was prepared by dissolving reagent-grade As_2O_3(s) in a NaOH solution. For a given set of experiments, the stock solutions of NaHS had the same sulfide concentration as the concentration of As in the stock sodium arsenite solutions. These two stock solutions were then mixed in various proportions to obtain solutions with ΣS/ΣAs ratios of 9, 5.25, 4, 3.17, 1.94, 1.00, 0.515, 0.25 and 0.11. Two different sets of experiments were carried out: one in which ΣAs + ΣS = 0.1 mol kg^{-1}, and one in which ΣAs + ΣS = 0.5 mol kg^{-1}. In each set of experiments, the pH of each of the solutions was adjusted to a constant value using solutions of NaOH or HCl. A pH range from 13.2 to approximately 7 was investigated. More acidic solutions could

DOI: 10.1039/b111453k

not be studied owing to precipitation of arsenic sulfide. Measurements of pH were conducted using an Orion Research Meter (Model SA250) with a Ross combination electrode, standardized against NIST pH buffers. An aliquot of each solution was placed in a glass NMR tube, and the tube was capped and sealed with Parafilm. The Raman spectrum of each solution was acquired at room temperature within 1–2 hours after being sealed in the NMR tube. Owing to the preliminary nature of the experiments, no internal standards were employed. Thus, the spectra could only be treated in a semi-quantitative manner.

The Raman instrumentation has been described in detail previously.[30,31] Raman spectra were excited using the 514-nm line of a Spectra Physics Ar-ion laser (model 2025-05) focused onto the sample with a cylindrical lens to match the monochromator slit. The laser delivered approximately 400 mW of power to the sample. The Raman scattering was viewed in a 135° backscattering configuration, with the scattered light collimated with a fast plano-convex lens (fl 1.3, planar side toward focused spot on sample) and then subsequently focused onto the slit of the monochromator (SPEX Triplemate, fl 6.3 input optics) with a second plano-convex f-matching lens (fl 6.5, planar side towards monochromator).The first two stages of the monochromator were locked in an additive–subtractive mode and function as a tunable bandpass filter, especially against the Rayleigh-scattered photons. The final stage dispersed the inelastically scattered photons across a Princeton Applied Research model 1420 intensified silicon diode-array detector. The slit width of the monochromator was set at 140 μm. In general, 10 scans, each with a 10 s integration time, were co-added to improve the signal-to-noise ratio. Spectra were calibrated against standard peaks of toluene in methanol and the emission lines of a neon lamp. Spectral data were saved as ascii files. Attempts to reduce the spectra in the manner described by Brooker *et al.*[32] or to use PeakFit (Jandel Scientific) to obtain quantitative band parameters (peak maxima, band widths, and band areas) were frustrated by the variable nature of the fluorescence of the NMR tube. Thus, only the raw spectra are presented here. However, PeakFit was employed to help identify the peaks of obvious Raman bands.

3. Results

Fig. 1 shows the background spectrum due to deionized water and the glass NMR tubes. The major features of the background are: (1) the Rayleigh wing descending from 250 cm^{-1}; (2) a broad, moderately intense, asymmetric band with a peak near 480 cm^{-1}; (3) a broad, weak band centered at 800 cm^{-1}; and (4) a very weak, broad band near 600 cm^{-1}. Water has libra- tion bands owing to hydrogen bonding at 450 and 789 cm^{-1} which may contribute to the two most prominent broad bands.[33] However, the broad band near 480 cm^{-1} is far more intense than usually observed in pure water, and probably is a result of fluorescence due to impurities in the glass NMR tube. The bands for thioarsenite species all fall on the low-wavenumber side of the broad band near 480 cm^{-1} which, combined with the proximity of the Rayleigh wing, hindered quantitative band-fitting.

Fig. 2–6 contain spectra for solutions containing both S and As. Each figure shows the spectra for a given pH and ΣS + ΣAs value as a function of ΣS/ΣAs ratio. For the convenience of the reader, some of these spectra are replotted in a slightly different manner in Fig. 7–11. In the latter, each figure shows the spectra for ΣS + ΣAs = 0.1 and a given ΣS/ΣAs ratio as a function of pH.

In our solutions with relatively high ΣS/ΣAs ratios, significant bisulfide (HS^-) is expected to be present. This species should yield a narrow band at about 2574 cm^{-1}.[34] At an early stage of this study, we verified that this band is present in some

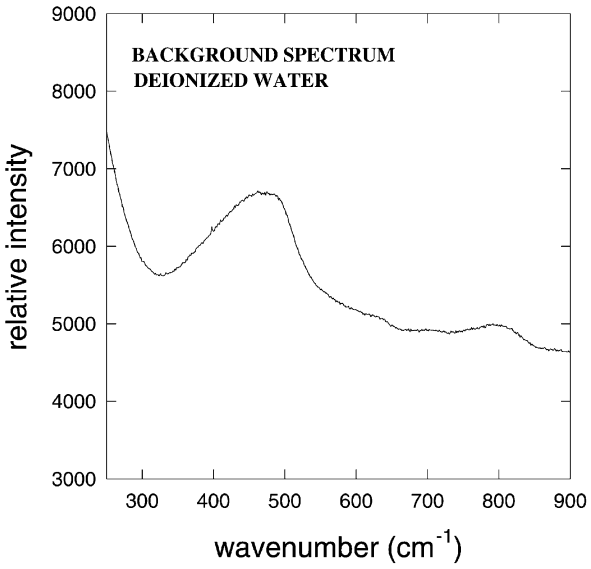

Fig. 1 Raman spectrum of deionized water in a glass NMR tube. Note broad bands from approximately 335 to 550 cm^{-1} and 750 to 850 cm^{-1}. There may also be a less intense broad band near 600 cm^{-1}.

of the solutions with higher ΣS/ΣAs ratios, but we did not routinely monitor this area of the spectrum. Attention was focused on the wavenumber range from 250 to 900 cm^{-1} where bands for thioarsenite and arsenite species occur.

Fig. 2 contains the spectra of solutions with ΣS + ΣAs = 0.1 mol kg^{-1} at pH = 13.2 for various ΣS/ΣAs ratios. At a ΣS/ΣAs ratio of 9, a prominent, narrow band centered at approximately 385 cm^{-1} is evident, together with a low-intensity shoulder on its high-wavenumber side. Upon a decrease in ΣS/ΣAs ratio to 5.25, another narrow band, centered near 400 cm^{-1} can be seen to emerge at the expense of the band at 385 cm^{-1}. The low-intensity shoulder on the high-wavenumber side does not appear to undergo much of a change as ΣS/ΣAs decreases. By a ΣS/ΣAs ratio of 4, the band at 385 cm^{-1} has disappeared. Between ΣS/ΣAs = 4 and ΣS/ΣAs = 0.25, the band at 400 cm^{-1} loses intensity, while a band

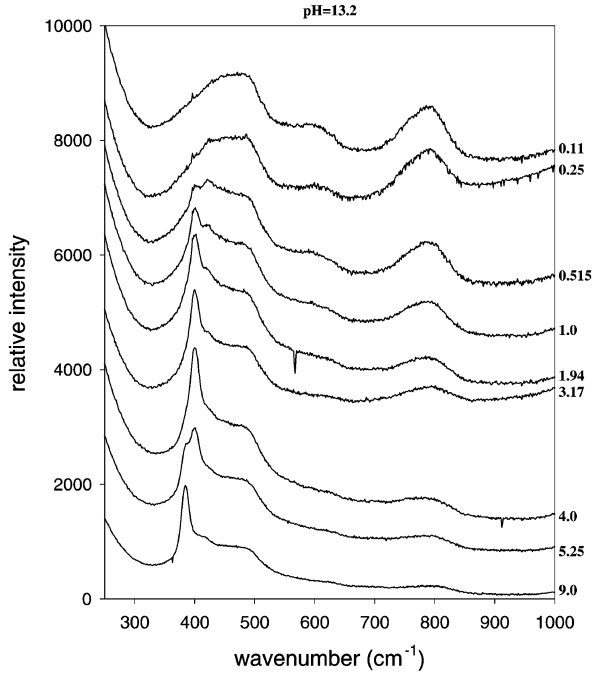

Fig. 2 Raman spectra of arsenic sulfide solutions at pH = 13.2 and ΣAs + ΣS = 0.1 mol kg^{-1} H_2O as a function of ΣS/ΣAs ratio.

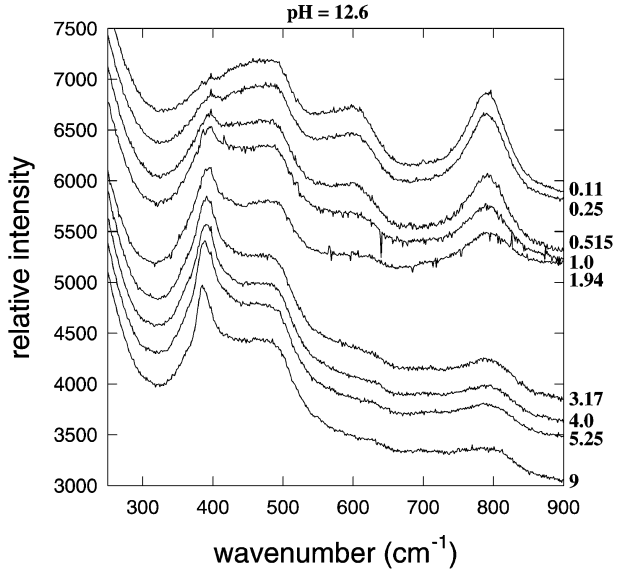

Fig. 3 Raman spectra of arsenic sulfide solutions at pH = 12.6 and ΣAs + ΣS = 0.1 mol kg^{-1} H_2O as a function of ΣS/ΣAs ratio.

centered near 420 cm^{-1} becomes relatively more prominent (although it never becomes very intense), until it too loses intensity. Meanwhile broad bands near 600 and 800 cm^{-1} grow in intensity. At ΣS/ΣAs = 0.11, the bands in the 350–450 cm^{-1} range have disappeared, leaving only the broad band observed in the background spectrum, and bands of increased intensity near 600 and 800 cm^{-1}. As indicated below, the increase in intensity of the latter bands can be attributed to the appearance of an arsenite species. It is possible that the shoulder observed on the high-wavenumber side of the bands at 385 and 400 cm^{-1} at higher ΣS/ΣAs ratios is the same as the band at 420 cm^{-1} visible at lower ΣS/ΣAs ratios, inasmuch as there continually appears to be some intensity at around 420 cm^{-1} throughout the entire range of ΣS/ΣAs ratios investigated. The bands at 385, 400 and 420 cm^{-1} each appear to belong to separate species as their intensities do not change in a concerted manner as ΣS/ΣAs is varied. Thus, at pH = 13.2 and ΣS + ΣAs = 0.1 mol kg^{-1} at least three separate species exist, in addition to that responsible for the bands at 600 and 800 cm^{-1}.

Raman spectra for solutions with ΣS + ΣAs = 0.1 mol kg^{-1}

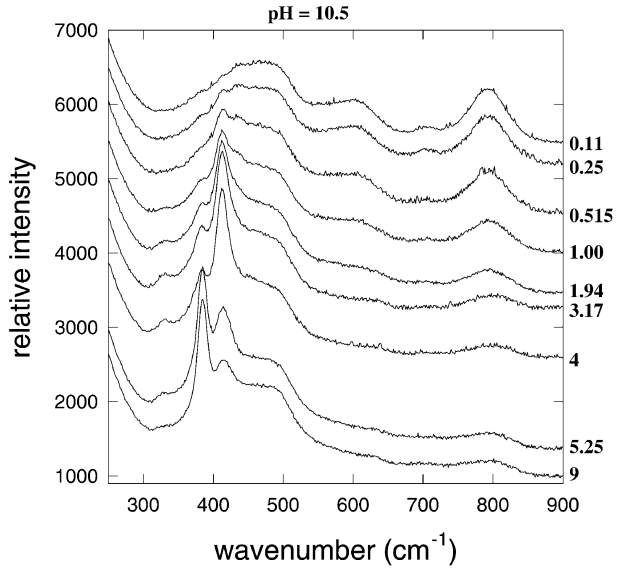

Fig. 4 Raman spectra of arsenic sulfide solutions at pH = 10.5 and ΣAs + ΣS = 0.1 mol kg^{-1} H_2O as a function of ΣS/ΣAs ratio.

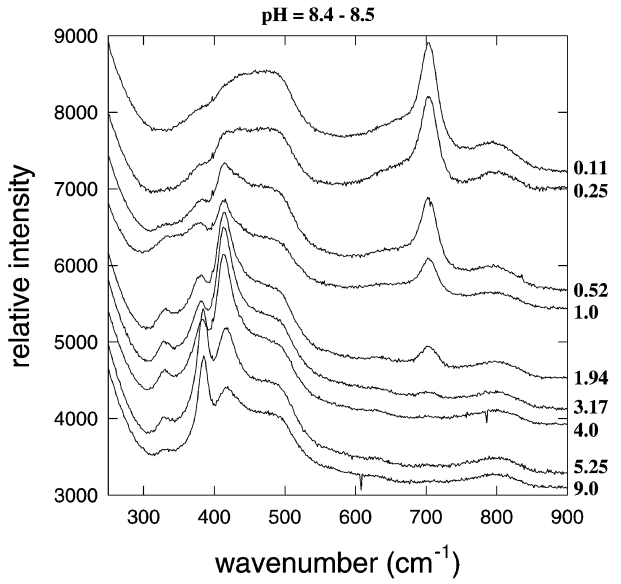

Fig. 5 Raman spectra of arsenic sulfide solutions at pH = 8.4–8.5 and ΣAs + ΣS = 0.1 mol kg^{-1} H_2O as a function of ΣS/ΣAs ratio.

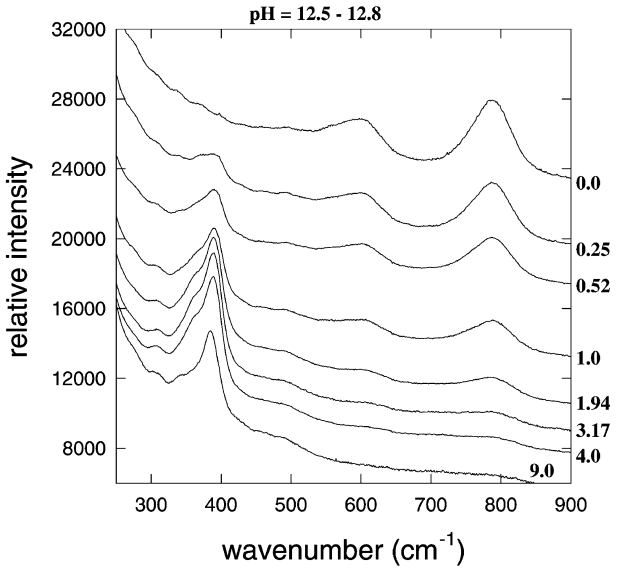

Fig. 6 Raman spectra of arsenic sulfide solutions at pH = 12.6 and ΣAs + ΣS = 0.5 mol kg^{-1} H_2O as a function of ΣS/ΣAs ratio.

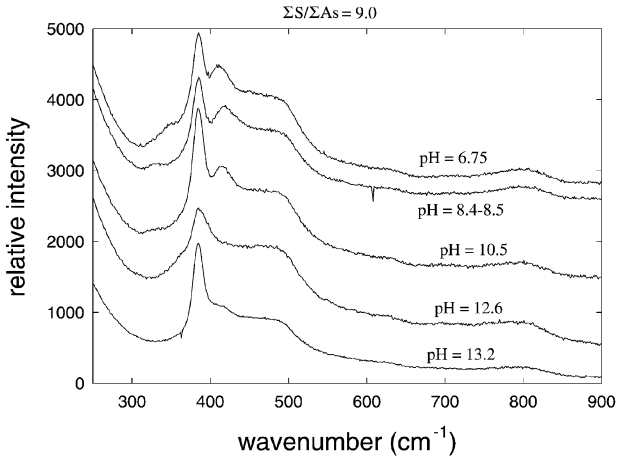

Fig. 7 Raman spectra of arsenic sulfide solutions at ΣS/ΣAs = 9.0 and ΣAs + ΣS = 0.1 mol kg^{-1} H_2O as a function of pH.

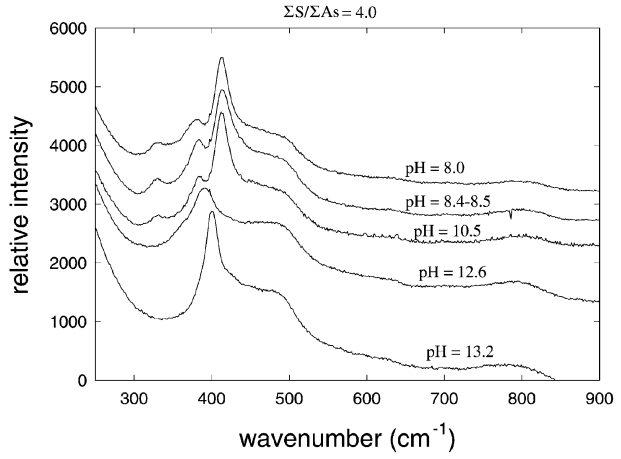

Fig. 8 Raman spectra of arsenic sulfide solutions at ΣS/ΣAs = 4.0 and ΣAs + ΣS = 0.1 mol kg^{-1} H_2O as a function of pH.

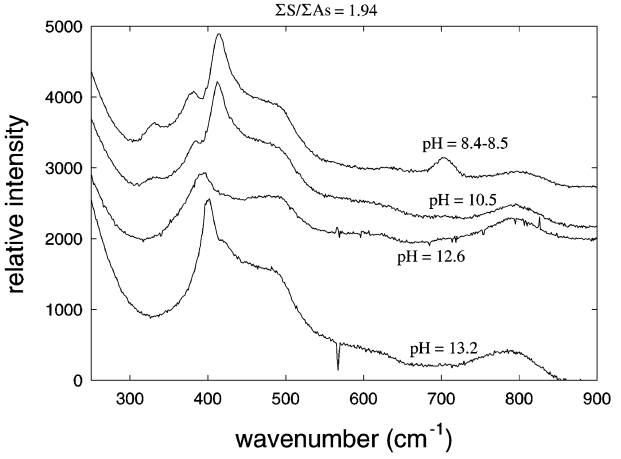

Fig. 9 Raman spectra of arsenic sulfide solutions at ΣS/ΣAs = 1.94 and ΣAs + ΣS = 0.1 mol kg^{-1} H_2O as a function of pH.

and pH = 12.6 are shown in Fig. 3. Only one prominent band is noted above background in the range 350–450 cm^{-1}, but the maximum of this band appears to shift from about 385 cm^{-1} to 397 cm^{-1} as the ΣS/ΣAs ratio varies from 9 to 0.25. The band is asymmetric to the high-wavenumber side, and there may also be some intensity above background on the low-wavenumber side. All of these observations suggest the presence of more

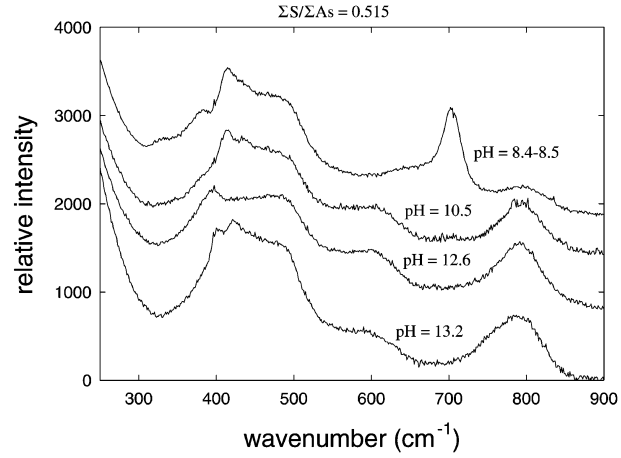

Fig. 10 Raman spectra of arsenic sulfide solutions at ΣS/ΣAs = 0.515 and ΣAs + ΣS = 0.1 mol kg^{-1} H_2O as a function of pH.

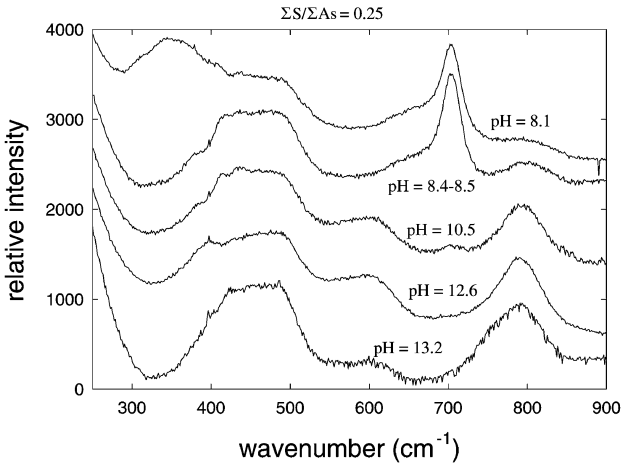

Fig. 11 Raman spectra of arsenic sulfide solutions at ΣS/ΣAs = 0.25 and ΣAs + ΣS = 0.1 mol kg^{-1} H_2O as a function of pH.

than one component to the band. We interpret these observations in terms of the presence of three strongly overlapping bands, the same ones at 385 and 400 cm^{-1} observed at pH = 13.2, and an additional band at approximately 390 cm^{-1}. The intensity of these bands varies with ΣS/ΣAs in such a manner that the apparent peak of the band envelope shifts to higher wavenumbers. As at pH = 13.2, as the ΣS/ΣAs ratio decreases, bands near 600 and 800 cm^{-1} increase in relative intensity, suggesting the formation of arsenite species.

The band near 385 cm^{-1}, observed in both Fig. 2 and 3, is also observed in solutions with high ΣS/ΣAs at ΣS + ΣAs = 0.1 mol kg^{-1} and pH = 10.5 (Fig. 4). In addition, at low ΣS/ΣAs ratios a band near 415 cm^{-1} is present, and this band increases in intensity with respect to the band at 385 cm^{-1} as ΣS/ΣAs decreases. A broad, low-intensity band appears to be present at about 330 cm^{-1} at ΣS/ΣAs = 9. This band increases and then seems to remain constant in intensity from ΣS/ΣAs = 5.25 to ΣS/ΣAs = 3.17, and then decreases in intensity and disappears by ΣS/ΣAs = 0.52. The band near 385 cm^{-1} remains visible until ΣS/ΣAs = 1, after which it disappears. The band at 415 cm^{-1} attains a maximum intensity at ΣS/ΣAs = 4, and then decreases in intensity until it disappears completely at ΣS/ΣAs < 0.25. The peak position of this band appears to change slightly from 415 to 412 cm^{-1} with decreasing ΣS/ΣAs ratio. A very low-intensity band appears at about 435 cm^{-1} at ΣS/ΣAs = 1.0 but disappears at ΣS/ΣAs < 0.25. At about ΣS/ΣAs = 1.94, bands begin to appear at 600 and 790 cm^{-1} and these grow in intensity to reach a maximum at the lowest ΣS/ΣAs (0.11) value measured. At ΣS/ΣAs < 0.515, a weak, broad band also appears near 700 cm^{-1}. The band near 415 cm^{-1} could possibly be interpreted to result from the same species responsible for the band observed at 420 cm^{-1} at pH = 13.2. However, we reject this interpretation for the following reasons: (1) A difference of 5–8 cm^{-1} is outside the uncertainty in identification of band peak positions for such a relatively narrow band; (2) the intensities of the bands at 330 and 415 cm^{-1} appear to be correlated, yet no corresponding band at 330 cm^{-1} was observed to occur with the band at 420 cm^{-1} at pH = 13.2 (although admittedly the intensity of the latter band is low and so a band at 330 cm^{-1} might not be detectable even if present); and (3) a band near 415–420 cm^{-1} was not observed at pH = 12.6, and it is highly unlikely that a species present at pH = 13.2 would first disappear and then reappear as pH decreases. Thus, we conclude that the band at 415 cm^{-1} represents a previously unidentified As species. The apparent shift of this band to lower wavenumbers with decreasing ΣS/ΣAs ratios could be an indication of overlap of bands of two different species, the relative intensities of which vary with ΣS/ΣAs ratio. The

apparent band at 435 cm^{-1} may represent yet another As species, but we are less confident of its existence because of the very low observed intensity of this band. Thus, at least one, possibly more, new species appear as pH is decreased to 10.5.

The spectra at low wavenumbers for solutions with $\Sigma S + \Sigma As = 0.1$ mol kg^{-1} and pH = 8.4–8.5 at high $\Sigma S/\Sigma As$ (Fig. 5) are very similar to those in Fig. 4 (pH = 10.5). Bands are observed near 330, 385 and 415 cm^{-1}, and the relative intensities of these bands at a given value of $\Sigma S/\Sigma As$ do not appear to be strongly dependent on pH. In fact, given the fact that pH differed by 2 units in the solutions the spectra of which are shown in Fig. 4 and 5, the lack of change in relative intensities of the bands in the region 300–450 cm^{-1} is particularly striking. On the other hand, the peak of the band near 415 cm^{-1} actually shifts from around 419 cm^{-1} at $\Sigma S/\Sigma As = 9.0$, to a minimum of 412 cm^{-1} at $\Sigma S/\Sigma As = 1.0$, and then back up to 415 cm^{-1} at $\Sigma S/\Sigma As = 0.52$. Once again, these apparent shifts may be an indication of the presence of two or more species with overlapping bands. In the spectral region above 500 cm^{-1} there are a number of changes that occur at low $\Sigma S/\Sigma As$ on going from pH = 10.5 to pH = 8.5. First, the intensity of the bands near 600 and 790 cm^{-1} are substantially reduced at the lower pH values. Second, a rather sharp band appears near 702 cm^{-1} and increases in intensity towards a maximum at $\Sigma S/\Sigma As = 0.11$. Finally, a low, broad shoulder appears on the low-wavenumber side of the latter peak at approximately 650 cm^{-1}.

Finally, Fig. 6 shows the spectra obtained for solutions with $\Sigma As + \Sigma S = 0.5$ mol kg^{-1} and pH = 12.5–12.8. At $\Sigma S/\Sigma As = 9.0$, these solutions exhibit an intense band with a peak near 384 cm^{-1} and asymmetric to the low-wavenumber side. Very weak peaks are also apparent at about 308 and 344 cm^{-1}. With decreasing $\Sigma S/\Sigma As$ ratio, the intense band near 384 cm^{-1} appears to shift to 389 cm^{-1}, and a prominent shoulder develops at ~365 cm^{-1}. The shoulder seems to maintain its intensity relative to the more intense band from $\Sigma S/\Sigma As = 4.0$ to 1.94. At lower $\Sigma S/\Sigma As$ ratios, both the shoulder near 365 and the main peak near 389 cm^{-1} decrease in intensity, but the intensity of the shoulder decreases faster than that of the main peak. At $\Sigma S/\Sigma As = 0.52$ the shoulder has all but disappeared, but the main band remains markedly asymmetric. This main band is still present at $\Sigma S/\Sigma As = 0.25$, but disappears completely at $\Sigma S/\Sigma As = 0$. Thus, at this higher value of $\Sigma As + \Sigma S$, at least one new species, one with a band near 365 cm^{-1}, has been identified. At this point is not clear whether the band near 308 cm^{-1} represents a separate species or is a band attributable to the same species responsible for the band at 365 cm^{-1}. However, the broadness of the spectral envelope in the region 350–400 cm^{-1} is permissive of the existence of several additional species. Very broad bands near 600 and 800 cm^{-1}, attributable to arsenite species, are clearly present at $\Sigma S/\Sigma As$ ratios as high as 1.94, and possibly 3.17. These are essentially the same bands observed in solutions with $\Sigma S + \Sigma As = 0.1$ mol kg^{-1} and pH = 12.6 at low $\Sigma S/\Sigma As$, indicating that the arsenite species do not form polynuclear species under the conditions investigated here. This conclusion is consistent with the Raman results of Pokrovski *et al.*[9] which showed that $H_3AsO_3^0$ does not form polynuclear species until $\Sigma As > 1$ mol kg^{-1}.

Fig. 7 shows the spectra at $\Sigma S + \Sigma As = 0.1$ and $\Sigma S/\Sigma As = 9.0$ as a function of pH. This figure shows essentially the same data as seen in Fig. 2–6, with the addition of the spectrum of a solution with pH = 6.75, the only solution of this pH for which we were able to obtain a spectrum. As discussed above, a band near 385 cm^{-1} persists at all pH values at the given values of $\Sigma S + \Sigma As$ and $\Sigma S/\Sigma As$. Moreover, a band near 415 cm^{-1} (accompanied by a band at 330 cm^{-1}) appears starting at pH = 10.5 and persists to the lowest pH investigated.

Spectra for $\Sigma S + \Sigma As = 0.1$ and $\Sigma S/\Sigma As = 4.0$ as a function of pH are compiled in Fig. 8. Again, these data were depicted in previous figures, with the exception of an additional spectrum collected at pH = 8.0. As noted previously, a band occurs at about 400 cm^{-1} at pH = 13.2, but by pH = 12.6, the latter is replaced by a band at ~390 cm^{-1}. At pH values between 10.5 and 8.0, bands occur at 330, 385 and 413 cm^{-1}, the relative intensities of which do not change much over a range of 2.5 pH units. Fig. 9 shows similar spectral features at $\Sigma S/\Sigma As = 1.94$ to those in Fig. 8, although at pH = 13.2 the band near 400 cm^{-1} seems to have a more prominent shoulder on its high-wavenumber side. Also, in Fig. 9 at pH = 8.4–8.5, a band appears at ~700 cm^{-1} as well.

At $\Sigma S + \Sigma As = 0.1$ and $\Sigma S/\Sigma As = 0.515$, the spectral features between 300 and 500 cm^{-1} (other than the background band) have very low intensities and are not very distinct (Fig. 10). Between pH = 10.5 and pH = 8.4–8.5, there is a notable change above 600 cm^{-1}, in which the broad band near 800 cm^{-1} gives way to a sharper band near 700 cm^{-1} that has a shoulder on the low-wavenumber side. At $\Sigma S + \Sigma As = 0.1$ and $\Sigma S/\Sigma As = 0.25$ (Fig. 11), the spectra are very similar to those in Fig. 10, except that there is almost no intensity above background from 300 and 500 cm^{-1}. Also, at pH = 8.1 a very broad band appears from about 300 to 420 cm^{-1}. This band most likely represents scattering from solid particles precipitated on decrease of pH.

The Raman bands enumerated above are the minimum number of bands present. There may well be other bands representing additional species, that cannot be resolved without quantitative band fitting. Indeed, results of attempts to perform such band fitting support the likely presence of other species. However, owing primarily to the presence and variable intensity of the broad fluorescence band, we found it impossible to fit the observed spectral data with bands that exhibited systematic peak positions, intensities and peak widths as a function of pH and $\Sigma S/\Sigma As$. Nevertheless, our results do indicate the presence of at least 6–8 separate S-bearing As species. It seems clear that separate species are responsible for bands near 365, 385, 390, 400, 415 (330) and 420 cm^{-1}. In addition, more tentatively identified bands at 308, 344 and 435 cm^{-1} may represent additional species (Table 1).

4. Discussion

Arsenite species

At low $\Sigma S/\Sigma As$ ratios, bands appear in the spectral region from 600 to 800 cm^{-1} which may be attributed to S-free, As(III) species (*i.e.*, arsenites). Loehr and Plane[35] have assigned Raman bands to the various arsenite species, and these assignments are given in Table 2. In Fig. 12, the distribution of arsenite species as a function of pH at 25 °C and 1 bar is illustrated.

The very broad bands observed near 600 and 800 cm^{-1} at pH = 13.2 (Fig. 2) are probably attributable to the species $HAsO_3^{2-}$ and AsO_3^{3-}, which are present in nearly equal proportions at pH = 13.2 (Fig. 12). The bands assigned by Loehr and Plane[35] to the first species are rather uncertain, but overall our observations are consistent with their band assignments for these two most deprotonated arsenite species.

At pH = 12.6 (Fig. 3 and 11), the bands at 600 and 800 cm^{-1} appear to be somewhat narrower than those at pH = 13.2, consistent with the predominance of a single species, $HAsO_3^{2-}$, at pH = 12.6 (Fig. 12). The positions of the bands are consistent with those given by Loehr and Plane[35] for $HAsO_3^{2-}$. The species $H_2AsO_3^-$ is expected to be predominant at pH = 10.5 according to the speciation diagram in Fig. 12. The spectral assignment of Loehr and Plane[35] would suggest the most intense bands for this species to occur at 790, 610, and 570 cm^{-1}. We observe the most intense band at 790 cm^{-1}, and a broad band that covers the region from 570 to 610 cm^{-1}, consistent with the predominance of $H_2AsO_3^-$ at this pH (Fig. 4 and 11). A weak band near 700 cm^{-1} is apparent at low

Table 1 Summary of observed Raman bands as a function of solution composition

ΣS + ΣAs/ mol kg^{-1}	pH	ΣS/ΣAs	Peak positions/cm^{-1}
0.1	13.2	9.0	385
		5.25	385, 400
		4.0	400
		3.17	400, 420, 600, 800
		1.94	400, 420, 600, 800
		1.0	400, 420, 600, 800
		0.52	400, 420, 600, 800
		0.25	420?, 600, 800
		0.11	600, 800
0.1	12.6	9.0	385
		5.25	389
		4.0	390
		3.17	391, 600, 800
		1.94	395, 600, 800
		1.0	395, 600, 800
		0.52	396, 600, 800
		0.25	397, 600, 800
		0.11	600, 800
0.1	10.5	9.0	385, 415
		5.25	327, 385, 415
		4.0	331, 385, 412
		3.17	332, 384, 413
		1.94	329, 384, 412, 600, 790
		1.0	329, 384, 412, 435?, 600, 790
		0.52	413, 435?, 600, 790
		0.25	435?, 600, 700, 790
		0.11	600, 700, 790
0.1	8.4–8.5	9.0	328, 385, 419
		5.25	329, 384, 418
		4.0	331, 384, 413
		3.17	331, 383, 413, 700
		1.94	332, 382, 414, 701
		1.0	334, 380, 412, 702
		0.52	333, 384, 415, 702, 800?
		0.25	415, ~650sh, 702, 800
		0.11	~650sh, 702, 800
0.1	6.75	9.0	~340, 385, 413
	8.0	4.0	331, 384, 413
	8.1	0.25	350, ~650sh, 702, 800
0.5	12.6	9.0	308, 344, 384
		4.0	308, 365sh, 389
		3.17	308, 365sh, 389
		1.94	308, 365sh,389, 600, 800
		1.0	308, 365sh,389, 600, 800
		0.52	308?, 390, 600, 800
		0.25	370?, 390, 600, 800
		0.11	600, 800

ΣS/ΣAs ratios in Fig. 4, which may be due to the presence of a small proportion of $H_3AsO_3^0$ at pH = 10.5 (*cf.* Fig. 12).

Finally, at pH $\leqslant$ 8.5, the speciation diagram in Fig. 12 suggests that the completely protonated arsenite, $H_3AsO_3^0$, should be predominant. For this species, Loehr and Plane,[35] and also Pokrovski *et al.*,[9] observed a very distinctive intense peak near 710 cm^{-1}, with a shoulder near 655 cm^{-1}. These features are clearly observed in Fig. 5, 10 and 11. We also observe a broad, low-intensity band near 790 cm^{-1} at pH = 8.5, which is consistent with the presence of a small proportion of $H_2AsO_3^-$ at pH = 8.5 (Fig. 12).

Table 2 Compilation of Raman spectral assignments for arsenite species from Loehr and Plane.[35]

Species[a]	Observed bands/cm^{-1}
$H_3AsO_3^0$ or $As(OH)_3^0$	710, 655
$H_2AsO_3^-$ or $AsO(OH)_2^-$	790, 610, 570, 370, 320
$HAsO_3^{2-}$ or $AsO_2(OH)^{2-}$	810?, 770?, 670-520?
AsO_3^{3-}	752, 680, 340

[a]Second formulations given are those preferred by Loehr and Plane.[35]

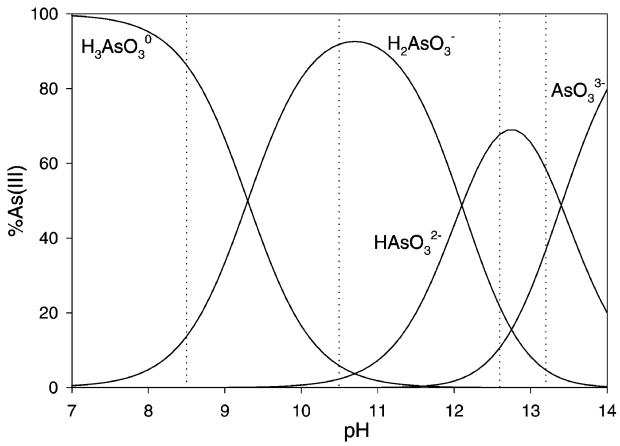

Fig. 12 Distribution of arsenite species as a function of pH at 25 °C and 1 bar. Thermodynamic data used to contruct this diagram (pK_1 = 9.3; pK_2 = 12.1; pK_3 = 13.4) are from Akinfiev *et al.*[8]

Thioarsenite species

The bands observed in the region 300–450 cm^{-1} can be attributed to As–S bonds.[24,36,37] These species may be simple thioarsenites, or a mixed species such as AsO_2S^{3-}, for example. However, as all the bands in the region above 500 cm^{-1} can be accounted for by known arsenite species, we will assume that simple thioarsenites are responsible for all the bands observed in the region 300–450 cm^{-1}. The Raman spectra offer evidence of the existence of at least 6–8 separate thioarsenite species over the range of conditions investigated. To simplify discussion, each major species (as inferred from the existence of a Raman band exhibiting independent behavior as a function of pH and ΣS/ΣAs) has been assigned an alphabetic designation as enumerated in the caption to Fig. 13. Fig. 13 summarizes the changes in species that occur as pH and ΣS/ΣAs ratio of the solution change. This diagram is highly schematic in that the positions and slopes of the boundaries among species are not

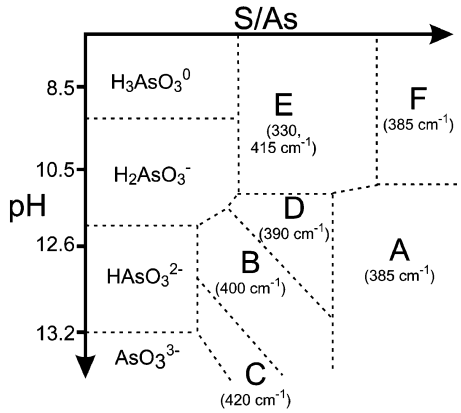

Fig. 13 Highly schematic diagram showing approximate predominance fields of various As species as a function of pH and ΣS/ΣAs ratio for ΣAs + ΣS = 0.1 mol kg^{-1} H_2O. With the exception of the boundaries between the arsenite species ($H_3AsO_3^0$, $H_2AsO_3^-$, $HAsO_3^{2-}$, AsO_3^{3-}), the slopes and the positions of the boundaries are highly uncertain. The letters correspond to species responsible for observed Raman bands as follows: A, 385 cm^{-1}; B, 400 cm^{-1}; C, 420 cm^{-1}; D, 390 cm^{-1}?; E, 330 and 415 cm^{-1}; and F, 385 cm^{-1}. At ΣAs + ΣS = 0.5 mol kg^{-1} H_2O an additional species with a band at 360–370 cm^{-1} joins species D at pH = 12.6 and intermediate ΣS/ΣAs.

well constrained. Furthermore, we cannot make any definitive statements regarding the exact stoichiometries of these thioarsenite species owing to a number of factors including: (1) the interference by fluorescence of the glass tubes employed; (2) absence of an internal standard; (3) lack of knowledge of the scattering coefficients of the various species; and (4) the relatively small number of bands that appear to be resolved for each species. However, a number of conclusions can be made regarding the chemical relationships among the various species indicated by the Raman bands.

If we assume that there is only a single species exhibiting a Raman band near 385 cm^{-1}, then the spectra show that species A occurs at the highest $\Sigma S/\Sigma As$ ratios at all pH values. At pH values of 13.2 and 12.6 and $\Sigma S + \Sigma As = 0.1$ mol kg^{-1}, species A appears to be the only or the greatly dominant thioarsenite present at $\Sigma S/\Sigma As = 9$, and other species begin to take its place as $\Sigma S/\Sigma As$ ratio decreases. At pH values of 10.5 and 8.5 and $\Sigma S + \Sigma As = 0.1$ mol kg^{-1}, or at pH = 12.6 and $\Sigma S + \Sigma As = 0.5$ mol kg^{-1}, species A is present at $\Sigma S/\Sigma As = 9$, but other species are present in significant proportion as well. In these cases also, species A is converted to other species as $\Sigma S/\Sigma As$ decreases. If indeed the band near 385 cm^{-1} arises from a single species, then these results suggest that species A is stable over a wide range of pH as long as $\Sigma S/\Sigma As$ is elevated.

Alternatively, the band near 385 cm^{-1} may contain contributions from more than one species that happen to have a Raman signal near this frequency. Some evidence for this interpretation comes from Fig. 7. Here it is seen that the band near 385 cm^{-1} appears to decrease in intensity from pH = 13.2 to pH = 12.6, but then increase again from pH = 12.6 to pH = 10.5. Although it is difficult to be certain whether these apparent changes in intensity are real in the absence of an internal standard, if so they suggest that possibly two different species exist with bands near 385 cm^{-1}. Moreover, at pH $\leqslant$ 10.5, bands at 385 and 415 cm^{-1} coexist, and their intensities seem to be quite insensitive to pH given a range of 3.75 units. One interpretation of the spectra in Fig. 7 is that a species (A) responsible for the band near 385 cm^{-1} at pH > 10.5 gives way to a second species (F) with a band near 385 cm^{-1} and one with a band near 415 cm^{-1} (E), the latter two having a pH-independent relationship to one another. This would account for the relative insensitivity of intensities of the two bands to pH at pH $\leqslant$ 10.5, while at the same time the initial appearance of the 415 cm^{-1} band is pH-dependent. The apparent near constant ratio of intensities of the bands 385 and 415 cm^{-1} above pH = 10.5 could imply that both bands arise from a single species. However, comparison of Fig. 7 and 8 shows that the relative intensities of these two bands, although insensitive to pH, are a strong function of the $\Sigma S/\Sigma As$ ratio, and thus cannot belong to the same species.

Fig. 13 shows that at $\Sigma S + \Sigma As = 0.1$ mol kg^{-1} and pH values of 8.5 and 10.5, species F converts to species E as the $\Sigma S/\Sigma As$ ratio decreases. Moreover, as mentioned in the Results section, the relative proportions of species F and E at a given $\Sigma S/\Sigma As$ ratio do not appear to be strongly dependent on pH (*cf.* Fig. 4, 5 and 7). These observations suggest that species A must possess a higher $\Sigma S/\Sigma As$ ratio than species E, but that there is no loss or gain of protons when species F converts to species E. Thus, the boundary between F and E has been drawn as a vertical, pH-independent boundary. On the other hand, species E is apparently destabilized on increasing pH to 12.6 and higher, whereupon species D, B and C appear in turn.

Species D appears only at pH = 12.6 at intermediate $\Sigma S/\Sigma As$ ratios. It is apparently present at both $\Sigma S + \Sigma As$ values investigated. Because the appearance of species D relative to E depends on the pH, species D may be a less protonated form of species E. As the $\Sigma S/\Sigma As$ ratio continues to decrease, species D is converted to species B.

At pH = 13.2, species A apparently converts directly to species B with decreasing $\Sigma S/\Sigma As$ ratio, without first going through species D, as was the case at pH = 12.6. With a further decrease in $\Sigma S/\Sigma As$ ratio, species C appears at the expense of species A and B.

Comparison to previous Raman studies of thioarsenite species

We are aware of only one other Raman study of aqueous thioarsenites—that of Helz *et al.*[24] The latter authors studied a solution containing 1 M NaHS and 0.08 M As ($\Sigma S/\Sigma As$ = 12.5) at pH 8.2 and 12 at 25 °C. They observed only three bands over the range 150–750 cm^{-1} at 325, 382 and 412 cm^{-1}. Upon an increase in pH from 8.2 to 12, the relative intensity of the band at 382 cm^{-1} increased at the expense of the two bands at 325 and 412 cm^{-1}. Based on *ab initio* calculations, Helz *et al.*[24] attributed the bands at 382 cm^{-1} to the species $AsS_2(HS)^{2-}$ and the bands at 325 and 412 cm^{-1} to the species $AsS(HS)_2^-$, which can be related to one another through the simple protonation reaction:

$$AsS_2(HS)^{2-} + H^+ \leftrightarrow AsS(HS)_2^-$$

In contrast, Fig. 4, 5 and 7 indicate that the situation may not be as simple. Like Helz *et al.*,[24] we note three bands in the pH range 8.5–10.5, at approximately 325, 382 and 412 cm^{-1} (in our case, 330, 385 and 415 cm^{-1}, *i.e.*, our species F and E), and we also observe generally a relative increase in the intensity of the band at 385 cm^{-1} with increasing pH at pH > 10.5 (the species responsible for the bands at 330 and 415 cm^{-1} disappears completely by pH = 12.6). However, we further observe that, at constant pH, the intensity of the band at 385 cm^{-1} decreases relative to that at 415 cm^{-1} with decreasing $\Sigma S/\Sigma As$ ratio. This observation indicates the existence of two species with different $\Sigma S/\Sigma As$ ratios. Moreover, the relative intensities of the bands at 385 and 415 cm^{-1} at constant $\Sigma S/\Sigma As$ ratio do not change very much with an increase of pH from 8.4 to 10.5 (Fig. 7). Over such a large pH range, if the species responsible for these bands were related simply by eqn. (1), we would expect much larger changes in relative intensity, as the ratio of concentrations of the species would have to change by one order of magnitude for each unit change in pH. Even in the work of Helz *et al.*,[24] the observed changes in relative intensities of the bands near 382 and 412 cm^{-1} as a function of pH were relatively small, even though pH was varied by nearly 4 units. If the only reaction occurring was reaction (1), there should have been a much greater change in relative intensities with a change in pH of this magnitude. Based on this reasoning, we are thus forced to conclude that at least three species exist at high $\Sigma S/\Sigma As$ over the pH range investigated. Two species (E and F), which differ only in their $\Sigma S/\Sigma As$ ratio but *not* their degree of protonation, exist at high $\Sigma S/\Sigma As$ and pH $\leqslant \sim 10.5$. As pH increases above 10.5, species E and F together give way to a single species A, which happens to yield a Raman band with a peak very similar to that of species F.

Helz *et al.*[24] provided a list of possible thioarsenite species and their predicted Raman shifts based on *ab initio* calculations. In principle, it should be possible to employ these calculated Raman frequencies to assign stoichiometries to each of the species observed in our study. However, we were unable to match the calculated frequencies of Helz *et al.*[24] to our observed Raman shifts and maintain consistency with the trends of the intensities of the spectral bands as a function of pH and $\Sigma S/\Sigma As$ ratio. We suspect that the main reason is that we have observed at least some species for which Helz *et al.*[24] do not give calculated Raman shifts. Moreover, considering the large number of species we have observed and how close their Raman shifts are, even small uncertainties in the shifts determined from *ab initio* calculations make it difficult to make definite assignments of species stoichiometry.

As(v) *vs.* As(iii)

In the above discussion, it has been assumed that the thioarsenic species present in our experiments contain arsenic in the As(iii) oxidation state. Mikenda *et al.*[37] report Raman bands for the As(v) species AsS_4^{3-} in the solid salt $Na_3AsS_4 \cdot 8H_2O$ and the band attributed to the symmetrical stretch of this species had a maximum at 385 cm^{-1}, which is very similar to the peak position for the band attributed in this study to species A. This raises the possibility that the arsenic in species A, and possibly other species, may be present in the As(v) oxidation state rather than the As(iii) state as assumed. In a Raman study of thioantimony species, Wood[38] similarly observed that the main thioantimony species in his solutions had bands with a maximum at approximately the same wavenumber as the Sb(v) species SbS_4^{3-} reported by Mikenda *et al.*[37] Finally, based on *ab initio* calculations Tossell[39] showed that calculated Raman stretching frequencies for Sb(iii)– and Sb(v)–sulfide complexes were very similar and do not permit a distinction among these two oxidation states based on Raman frequencies alone. However, Wood[38] (1989) was able to rule out the presence of a significant concentration of SbS_4^{3-} based on the polarization behavior of the Raman bands. On the other hand, others[40,41] have presented EXAFS evidence that aqueous Sb(v)–sulfide species are produced when the Sb(III)–solid Sb_2S_3 reacts with aqueous bisulfide.

In the experiments described here, arsenic is clearly in the As(iii) form at low ΣS/ΣAs ratios where Raman spectra characteristic of arsenite species were obtained. Sulfide-free solutions containing As(iii) were mixed with deoxygenated bisulfide solutions to produce the solutions at high ΣS/ΣAs where thioarsenic species were observed. If these thioarsenic species contain As(v), this implies that oxidation of As(iii) occurred upon mixing with the reduced bisulfide solution and formation of the thioarsenic complexes. The question then becomes, what is the oxidant in the reaction? It seems unlikely to be dissolved oxygen, owing to the care taken to exclude this gas during the preparation of the solution. Moreover, even if the solutions were saturated with oxygen, this would result in an O_2 concentration of no more than 10 mg kg^{-1}, or 3.1×10^{-4} mol kg^{-1}. The lowest As concentration in any of the solutions employed was 0.01 mol kg^{-1}, so even in a solution saturated in oxygen, there would be too little oxygen available to oxidize all the As(iii) initial present. Because all solutions were prepared from degassed water and were handled in an inert atmosphere, the oxygen content should be much lower than 10 mg kg^{-1}, and any residual oxygen left should be scavenged by the bisulfide in the solutions with high ΣS/ΣAs ratios.

In order to explain the oxidation of Sb(iii) to Sb(v) in their study, Mosselmans *et al.*[40] proposed the following reaction:

$$(y + 1 - x)H^+ + HS^- + H_xSbS_3^{(x-3)} \leftrightarrow H_ySbS_4^{(y-3)} + H_2(g)$$

In this case, H^+ is the oxidant. Reaction (2) suggests that, except in the special case where $x = 1 + y$, substantial shifts in pH should be observed as oxidation occurs, unless the solution is buffered. Thus, if a similar oxidation reaction occurred in our study of As–sulfide species, we should have seen a strong shift in pH as oxidation proceeded. During the preparation of solutions, we did not note any drift in pH, nor did we observe the effervescence of any gases, which could be attributed to production of hydrogen. We cannot rule out the possibility that a pH change occurred in the solution after it was sealed in the capillary tube, but evolution of hydrogen also was not observed after the solution was sealed in the tube. Thus, we feel justified in assuming the presence of As(iii)–sulfide species. However, future investigations of this system should take steps to determine definitively the oxidation state of As in these thioarsenic complexes.

Moreover, recently Jayanetti *et al.*[42] have shown that oxidation–reduction reactions can occur during EXAFS measurements owing to the radiolysis of water by intense synchrotron X-ray beams to produce H_2 and O_2. There is therefore the possibility that in the EXAFS studies,[40,41] oxidation of Sb(iii) to Sb(v) occurred during measurements as a result of radiolysis. It seems only fair to mention that oxidation–reduction reactions could also be triggered by intense photon beams such as those employed in laser Raman spectroscopy. The resolution of the oxidation state of As and Sb in thio-complexes may require techniques that do not involve intense beams of electromagnetic radiation.

Implications

Although we can not identify unambiguously the stoichiometries of the thioarsenite species present in our experiments, our results do have some important implications. Our study clearly demonstrates the complexity of the As–S–O–H system in that a relatively large number of species may be present. We have definitive proof of the existence of at least 6 or 7 different thioarsenic species in addition to the various arsenite species, and there may well be more species present that we could not resolve owing to peak overlap. Although detailed band fitting may change the details of our interpretations, our data clearly show the presence of a relatively large number of thioarsenite species. It may be this degree of complexity which explains the discrepancies in interpretations of previous studies. Our study also has implications for EXAFS investigations of such systems. EXAFS is a very powerful technique for the study of species in aqueous solution, but it provides a measure of the average coordination of an element in solution. Where several species exist simultaneously in significant concentrations, the interpretation of EXAFS results may not be straightforward. Thus, it may be necessary that a technique that can "see" individual species, such as Raman spectroscopy, be used in conjunction with EXAFS. Also, the possibility of radiolytic oxidation/reduction EXAFS measurements must be taken into account when making EXAFS measurements on redox-sensitive systems.

Acknowledgement

This research was funded in part by a grant to SAW from Barrick Goldstrike, administered by the Bureau of Land Management. SAW also acknowledges receipt of two summer faculty research fellowships from AWU-DOE (Associated Western Universities – Department of Energy). CDT and DRJ were supported by DOE – Basic Energy Sciences, Division of Engineering and Geosciences. Two *Geochemical Transactions* referees are thanked for their helpful comments.

References

1 R. Höltje, *Z. Anorg. Chem.*, 1929, **181**, 395.
2 R. Nagakawa, *Nippon Kagaku Zasshi*, 1971, **92**, 154.
3 A. A. Ivakin, S. Vorob'eva, E. M. Gertman and E. M. Voronova, *Russ. J. Inorg. Chem.*, 1976, **21**, 237.
4 G. D. Mironova, A. Zotov and N. I. Gul'ko, *Geochem. Int.*, 1984, **21**, 53.
5 C. A. Heinrich and P. J. Eadington, *Econ. Geol.*, 1986, **81**, 511.
6 J. M. Ballantyne and J. N. Moore, *Geochim. Cosmochim. Acta*, 1988, **52**, 475.
7 J. Webster, *Geochim. Cosmochim. Acta*, 1990, **54**, 1009.
8 N. N. Akinfiev, A. Zotov and A. Nikonorov, *Geochem. Int.*, 1992, **29**, 109.
9 G. Pokrovski, R. Gout, J. Schott, A. Zotov and J.-C. Harrichoury, *Geochim. Cosmochim. Acta*, 1996, **60**, 737.
10 A. Criaud and C. Fouillac, *Geochim. Cosmochim. Acta*, 1986, **50**, 1573.
11 M. H. Wünschendorff, *Bull. Soc. Chim. Fr.*, 1929, **45**, 897.
12 A. K. Babko and G. S. Lisetskaya, *Russ. J. Inorg. Chem.*, 1956, **1**, 95.

13 M. H. N. Srivastava and S. Ghosh, *Proc. Natl. Acad. Sci., India*, 1957, **26**, section E, part III, 250.
14 M. H. N. Srivastava and S. Ghosh, *J. Ind. Chem. Soc.*, 1958, **35**, 1659.
15 J. Angeli and P. Souchay, *Compt. Rend. Acad. Sci., Paris*, 1960, **250**, 713.
16 B. G. Weissberg, *Geochim. Cosmochim. Acta*, 1966, **30**, 815.
17 R. W. J. Raab, PhD Thesis, University of California, Riverside, 1969.
18 S. V. Vorob'eva and A. A. Ivakin, *Russ. J. Inorg. Chem.*, 1977, **22**, 1479.
19 A. A. Ivakin, S. Vorob'eva, A. M. Gorelov and E. M. Gertman, *Russ. J. Inorg. Chem.*, 1979, **24**, 1089.
20 G. D. Mironova and A. Zotov, *Geochem. Int.*, 1980, **17**, 46.
21 N. F. Spycher and M. H. Reed, *Geochim. Cosmochim. Acta*, 1989, **53**, 2185.
22 G. D. Mironova, A. Zotov and N. I. Gul'ko, *Geochem. Int.*, 1990, **27**, 61.
23 L. E. Eary, *Geochim. Cosmochim. Acta*, 1992, **56**, 2267.
24 G. R. Helz, J. A. Tossell, J. M. Charnock, R. A. D. Pattrick, D. J. Vaughan and C. D. Garner, *Geochim. Cosmochim. Acta*, 1995, **59**, 4591.
25 N. F. Spycher and M. H. Reed, *Geochim. Cosmochim. Acta*, 1990, **54**, 3241.
26 N. F. Spycher and M. H. Reed, *Geochim. Cosmochim. Acta*, 1990, **54**, 3246.
27 R. E. Krupp, *Geochim. Cosmochim. Acta*, 1990, **54**, 3239.
28 R. E. Krupp, *Geochim. Cosmochim. Acta*, 1990, **54**, 3245.
29 R. E. Krupp, *Geochim. Cosmochim. Acta*, 1988, **52**, 3005.
30 N. A. Marley, M. Ott, B. L. Feary, T. M. Benjamin, P. S. Z. Rogers and J. S. Gaffney, *Rev. Sci. Instrum.*, 1988, **59**, 2247.
31 C. D. Tait, D. R. Janecky and P. S. Z. Rogers, *Geochim. Cosmochim. Acta*, 1991, **55**, 1253.
32 M. H. Brooker, G. Hancock, B. C. Rice and J. Shapter, *J. Raman Spectrosc.*, 1989, **20**, 683.
33 G. E. Walrafen, *J. Chem. Phys.*, 1962, **36**, 1035.
34 B. Meyer, K. Ward, K. Koshlap and L. Peter, *Inorg. Chem.*, 1983, **22**, 2345.
35 T. M. Loehr and R. A. Plane, *Inorg. Chem.*, 1968, **7**, 1708.
36 A. Rogstad, *J. Mol. Struct.*, 1972, **14**, 421.
37 W. Mikenda, H. Steidl and A. Preisinger, *J. Raman Spectrosc.*, 1982, **12**, 217.
38 S. A. Wood, *Geochim. Cosmochim. Acta*, 1989, **53**, 237.
39 J. A. Tossell, *Geochim. Cosmochim. Acta*, 1994, **58**, 5093.
40 J. F. W. Mosselmans, G. R. Helz, R. A. D. Pattrick, J. M. Charnock and D. J. Vaughan, *Appl. Geochem.*, 2000, **15**, 879.
41 D. M. Sherman, K. V. Ragnarsdottir and E. H. Oelkers, *Chem. Geol.*, 2000, **167**, 161.
42 S. Jayanetti, R. A. Mayanovic, A. J. Anderson, W. A. Bassett and I.-M. Chou, *J. Chem. Phys.*, 2001, **115**, 954.